AGU PUBLICATIONS

Geophysical Research Letters

RESEARCH LETTER
10.1002/2014GL061600

Key Points:
- The meltwater from Amundsen Sea ice shelves flows into the Ross Sea
- A slight ice loss increase can strongly intensify meltwater transport
- The mechanism purposed in this study may explain the Ross Sea freshening

Supporting Information:
- Readme
- Tables S1–S3

Correspondence to:
Y. Nakayama,
Yoshihiro.Nakayama@awi.de

Citation:
Nakayama, Y., R. Timmermann, C. B. Rodehacke, M. Schröder, and H. H. Hellmer (2014), Modeling the spreading of glacial meltwater from the Amundsen and Bellingshausen Seas, *Geophys. Res. Lett.*, *41*, 7942–7949, doi:10.1002/2014GL061600.

Received 17 SEP 2014
Accepted 1 NOV 2014
Accepted article online 6 NOV 2014
Published online 24 NOV 2014

Modeling the spreading of glacial meltwater from the Amundsen and Bellingshausen Seas

Y. Nakayama[1], R. Timmermann[1], C. B. Rodehacke[2], M. Schröder[1], and H. H. Hellmer[1]

[1]Alfred Wegener Institute, Bremerhaven, Germany, [2]Danish Meteorological Institute, Copenhagen, Denmark

Abstract It has been suggested that an increased melting of continental ice in the Amundsen Sea (AS) and Bellingshausen Sea (BS) is a likely source of the observed freshening of Ross Sea (RS) water. To test this hypothesis, we simulate the spreading of glacial meltwater using the Finite Element Sea Ice/Ice Shelf/Ocean Model. Based on the spatial distribution of simulated passive tracers, most of the basal meltwater from AS ice shelves flows toward the RS with more than half of the melt originating from the Getz Ice Shelf. Further, the model results show that a slight increase of the basal mass loss can substantially intensify the transport of meltwater into the RS due to a strengthening of the melt-driven shelf circulation and the westward flowing coastal current. This supports the idea that the basal melting of AS and BS ice shelves is one of the main sources for the RS freshening.

1. Introduction

The ice shelves and glaciers of the West Antarctic Ice Sheet (WAIS) are thinning rapidly especially in the Amundsen Sea (AS) and Bellingshausen Sea (BS) [e.g., *Pritchard et al.*, 2012; *Shepherd et al.*, 2012; *Rignot et al.*, 2013]. This is mainly caused by strong basal melting due to the interaction of deep-drafted ice shelves with warm Circumpolar Deep Water (CDW, about 3°C warmer than the in situ freezing point) flowing onto the continental shelves through submarine glacial troughs [e.g., *Jacobs et al.*, 2011; *Pritchard et al.*, 2012]. Basal mass loss of the AS and BS ice shelves is estimated to be ~500 and 150 Gt yr^{-1}, respectively, according to satellite analyses [*Rignot et al.*, 2013]. This is about half of the total basal melting of all Antarctic ice shelves [*Depoorter et al.*, 2013; *Rignot et al.*, 2013].

In the Ross Sea (RS), shelf water salinity has declined by 0.03 per decade over the past 50 years [*Jacobs et al.*, 2002; *Jacobs and Giulivi*, 2010]. Since the freshening may be responsible for a change in the characteristics of the Antarctic Bottom Water formed in the RS [*Jacobs et al.*, 2002; *Rintoul*, 2007] and thus may influence the global thermohaline circulation, understanding that the possible link between the melting of West Antarctic ice shelves and the freshening of the RS is crucial for assessing climate change in the Southern Ocean. Although changes in precipitation, sea ice production, and ocean circulation are considered to be possible reasons for the freshening, increased melting of continental ice upstream in the AS and BS is suggested to be the likely source of the additional freshwater [*Jacobs et al.*, 2002; *Jacobs and Giulivi*, 2010]. The salinity of the westward flowing coastal current into the RS has decreased by 0.08 per decade over the past 30 years, and oxygen isotope data of the shelf water show an increasing glacial melt signal, supporting this hypothesis [*Jacobs and Giulivi*, 2010].

Although high-resolution circumpolar or global models resolving all the small ice shelves of the WAIS are required to study this hypothesis, it has been difficult to simulate the CDW intrusions onto the AS and BS continental shelves in these models [*Timmermann et al.*, 2012; *Kusahara and Hasumi*, 2013]. However, *Nakayama et al.* [2014] successfully reproduced the CDW intrusions onto the continental shelf and basal mass loss rates of the major AS and BS ice shelves using the global Finite Element Sea Ice/Ice Shelf/Ocean Model (FESOM) [*Timmermann et al.*, 2012]. In this study, we simulate the spreading of basal meltwater from the AS and BS ice shelves using FESOM and investigate whether the basal meltwater from these ice shelves flows into the RS. We also conduct two sensitivity experiments, assessing this hypothesis, and discuss the sensitivity of basal meltwater transport into the RS to the strength of the basal mass loss of AS and BS ice shelves.

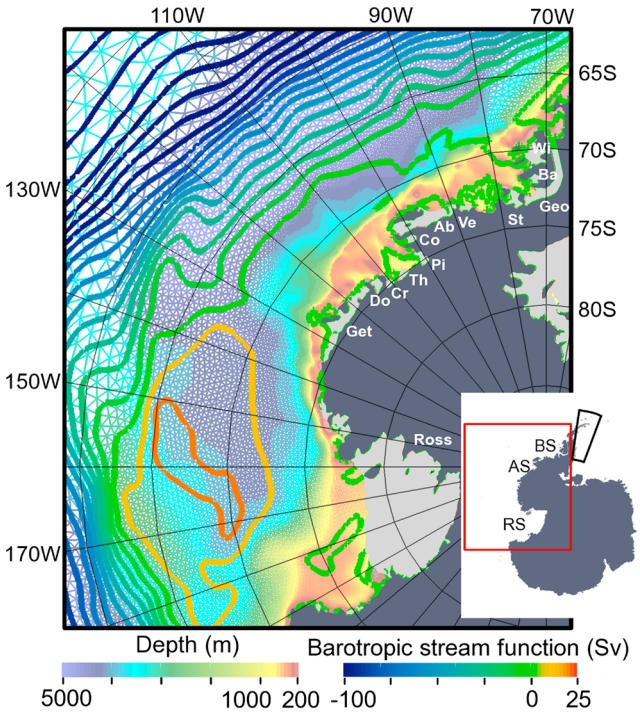

Figure 1. Horizontal grid of the AS, BS, and RS regions of the global model with the depth of the model bathymetry (color) and simulated mean barotropic stream function in the CTRL case (thick contours with contour interval of 10 Sv). The inset (right bottom) shows Antarctica with regions surrounded by red and black lines denoting the location of the enlarged portion and the location where temperature and salinity are restored (black box), respectively. Locations of ice shelves are shown with acronyms that are summarized in Table S1 in supporting information.

2. Model

We use the global FESOM, the details of which are described in *Timmermann et al.* [2009, 2012], *Timmermann and Hellmer* [2013], and *Nakayama et al.* [2014]. We use a tetrahedral mesh with a horizontal spacing of 100 km along non-Antarctic coasts, which is refined to ~20 km along the Antarctic coast, 10–20 km under the large ice shelves in the RS, ~5 km in the central AS and BS and ~2.5 km in the eastern AS (Figure 1). To allow for an adequate representation of ice shelf cavities, we apply a hybrid vertical coordinate system with 46 layers and a *z* level discretization in the middle- and low-latitude ocean basins. The top 21 layers along the Antarctic coast are terrain-following (sigma coordinate) for depths shallower than 650 m [*Nakayama et al.*, 2014, Figure 2]. In the *z* coordinate region (open ocean), bottom nodes are allowed to deviate from their nominal layer depth in order to allow for a correct representation of bottom topography, similar to the shaved-cell approach in finite difference models. Ice shelf cavity geometry, and global ocean bathymetry have been derived from the RTopo-1 data set [*Timmermann et al.*, 2010]. Ocean bathymetry of the AS, BS, and RS regions of the global model is shown in Figure 1. A Gaussian function with a width depending on the model's horizontal resolution is applied to smooth ice shelf draft and seafloor topography in the sigma-coordinate region.

Following *Timmermann et al.* [2012], we assume a steady state for ice shelf thickness and cavity geometry and compute basal mass loss rate at ice shelf bases as proposed by *Hellmer and Olbers* [1989] and refined by *Holland and Jenkins* [1999]. Turbulent fluxes of heat and salt are computed with coefficients depending on the friction velocity, following *Jenkins* [1991]. To trace the basal meltwater, we do not implement geochemical tracers [*Rodehacke et al.*, 2007], but we use virtual passive tracers, which are released at the same rate as melting occurs at the ice shelf bases. Several independent virtual passive tracers are used to identify detailed pathways of basal meltwater from the different ice shelves in the AS and BS.

For this study, we force the model with 6-hourly atmospheric data from the National Centers for Environmental Prediction Climate Forecast System Reanalysis [*Saha et al.*, 2010] for the period 1979–1988. The model is spun-up for 5 years by repeating the 1979 forcing, because ice shelf basal mass loss for most ice shelves approaches a quasi-steady state within the first 5 years of integration [*Timmermann et al.*, 2012]. Initial temperature and salinity are derived from the World Ocean Atlas 2001 [*Conkright et al.*, 2002] January mean data set. In addition, temperature and salinity are restored to the initial values with a time scale of 30 days in the vicinity of Antarctic Peninsula at depths deeper than 150 m (sector indicated by the black line in the top left of Figure 1), because too coarse vertical and horizontal resolutions there do not allow for the descent of dense water to great depths.

3. Results

3.1. Model Validation

As shown for slightly different configurations in *Timmermann et al.* [2012] and *Timmermann and Hellmer* [2013], the model reproduces many features of ocean circulation and sea ice distribution in good

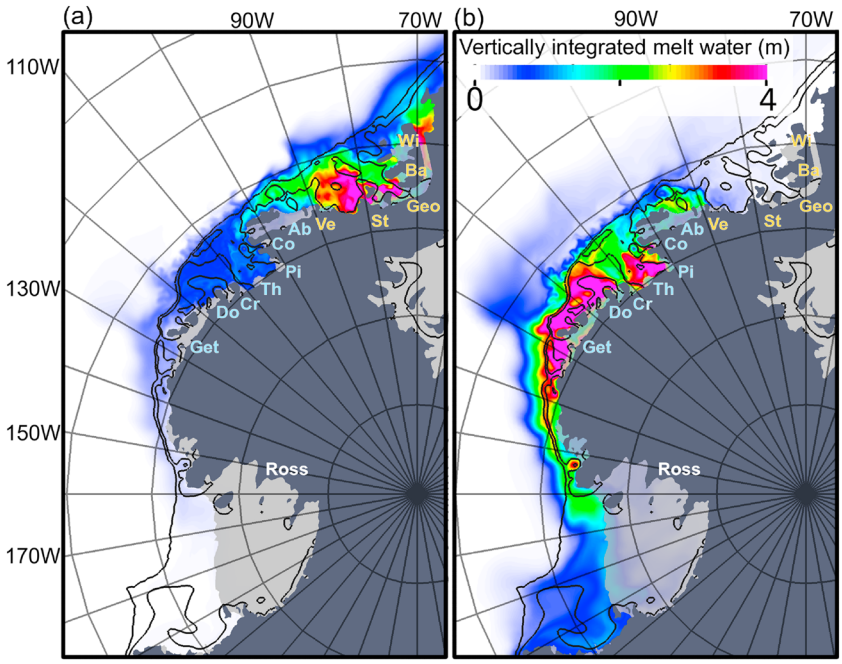

Figure 2. Spatial distributions of vertically integrated meltwater content after 10 years of simulation showing the basal meltwater from (a) ice shelves in the BS (names in light yellow) and (b) ice shelves in the AS (names in light blue). The bathymetry contours of 500 and 1000 m are shown (black lines). Locations of ice shelves are indicated by acronyms that are summarized in Table S1 in the supporting information.

agreement with observations. In the configuration used here, e.g., the transport of the Ross Gyre is ~26 Sv and the Antarctic Circumpolar Current (ACC) carries ~140 Sv through Drake Passage (Figure 1). For the AS, BS, and RS regions (160°E–70°W), the modeled winter (September) sea ice extent is similar to observations [*Cavalieri et al.*, 2006], while summer (March) sea ice extent is overestimated by ~24%. However, the spatial distribution of summer sea ice is now closer to reality with more sea ice remaining in the AS and BS compared to *Timmermann et al.* [2012] (not shown). The model results show CDW intrusions through submarine glacial troughs into the ice shelf cavities, consistent with observations and regional model studies [*Jacobs and Giulivi*, 2010; *Schodlok et al.*, 2012; *Assmann et al.*, 2013; *Nakayama et al.*, 2013; *Walker et al.*, 2013], and simulated mean bottom temperature and salinity in the AS and BS are mostly close to near-bottom conductivity-temperature-depth observations [*Nakayama et al.*, 2014, Figure 4]. Modeled meltwater fractions are about 1–2 % at the southern George VI and Pine Island Ice Shelf fronts at a depth of ~200 m, which is also consistent with observations [*Jenkins and Jacobs*, 2008; *Jacobs et al.*, 2011; *Nakayama et al.*, 2013].

There are several studies estimating the basal mass loss of West Antarctic ice shelves based on satellite, glaciological, and oceanographic observations [e.g., *Jacobs et al.*, 2011; *Depoorter et al.*, 2013; *Rignot et al.*, 2013]. After the spin-up phase, modeled basal mass loss is nearly stable throughout the integration [*Nakayama et al.*, 2014]. For the ice shelves in the AS and BS, the rates of total basal mass loss are 262 Gt yr^{-1} and 162 Gt yr^{-1}, respectively, which are consistent with the observation-based estimates (Table S1 in the supporting information). For the individual ice shelves in the AS and BS, modeled basal mass loss rates are mostly within or close to the ranges of observation-based estimates [e.g., *Potter et al.*, 1984; *Corr et al.*, 2002; *Jacobs et al.*, 2011; *Depoorter et al.*, 2013; *Rignot et al.*, 2013] (Tables S1 and S2 in the supporting information). The differences are large, however, for the Thwaites, Crosson, and Doston Ice Shelves, where the modeled (observed) basal mass loss is 27 (91–105), 3.3 (35–43), and 20 (41–49) Gt yr^{-1}, respectively. The modeled basal mass loss of Pine Island Ice Shelf is slightly lower than the lower bound of the observation-based estimates, and it is highly underestimated when compared to the estimates from *Jacobs et al.* [2011], *Depoorter et al.* [2013], and *Rignot et al.* [2013]. These discrepancies may be caused by modeled CDW intrusions still being too weak [*Nakayama et al.*, 2014] and ice front temperatures still being lower than observed (e.g., ~0.5°C lower at the Pine Island Ice Shelf front). It is also possible that the *Rignot et al.* [2013] estimates, using the volume flux divergence of ice shelves in 2007 and 2008, are biased toward higher values. For Pine Island Ice Shelf, *Rignot et al.* [2013] estimate is close to the upper bound of the observation-based estimates

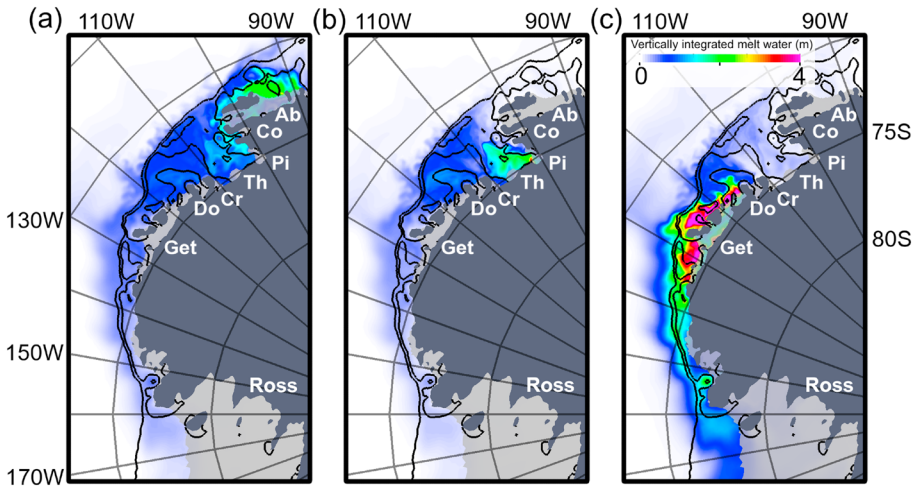

Figure 3. Same as Figure 2 but showing the spatial distributions of the basal meltwater from (a) Abbot Ice Shelf, (b) Pine Island Ice Shelf, and (c) Getz Ice Shelf after 10 years of simulation.

(Table S2 in the supporting information). It is also known that the basal mass loss of Pine Island Ice Shelf decreased to less than half of the estimate from *Rignot et al.* [2013] in summer 2012 [*Dutrieux et al.*, 2014]. For ice shelves in the RS (Land, Nickerson, Sulzberger, Swinburne, and Ross Ice Shelves), the total basal mass loss is 159 Gt yr^{-1}, which is overestimated by ~25–50% compared to the observation-based estimate. However, our results are closer to reality compared to the results from *Timmermann et al.* [2012].

Although there are some differences between our model results and observations, we are able to reproduce warm CDW intrusions and basal melting of ice shelves in the AS and BS. Thus, we refer to this as the CTRL case.

3.2. Spreading of the Basal Meltwater From West Antarctic Ice Shelves

After 10 years of simulation, about 70% of the basal meltwater from the BS flows westward, while the rest flows northeastward (east of 70°W) along the path of the ACC (Figure 2a). For the basal meltwater from the BS, 16% reaches the AS (west of 100°W), and only 2% reaches the RS (west of 134°W). On the other hand, basal meltwater from the AS mostly flows westward with 36% reaching the RS (Figure 2b). Investigating the four largest sources, the basal meltwater from the George VI Ice Shelf spreads both eastward and westward (not shown) but is very similar to Figure 2a. The meltwater from the Abbot and Pine Island Ice Shelves flows westward, but only 20% and 25% reaches the RS, respectively (Figures 3a and 3b). The meltwater from the Getz Ice Shelf flows westward and more than 50% influences the RS (Figure 3c). For the amount of basal meltwater from the AS and BS in the RS (160°E–134°W), 95% (5%) originates from the AS (BS). The basal meltwater in the RS originating from the AS consists of 58% from the Getz, 8% from the Pine Island, and 11% from the Abbot Ice Shelves, respectively. This confirms the importance of the Getz Ice Shelf for the meltwater transport into the RS, as also suggested by *Jacobs et al.* [2013]. However, we note that the contributions of Pine Island Ice Shelf and Thwaites Glacier may be underestimated in our model, because the simulated basal mass losses are too small for these ice shelves.

In contrast, *Kusahara and Hasumi* [2014], who investigated the spreading of meltwater from all Antarctic ice shelves, show that most of the basal meltwater originating from the AS and BS flows eastward along the path of the ACC. However, since their focus was rather on East Antarctica with coarser resolution in the AS and BS (~20 km), CDW intrusions and ice shelf basal melting in these regions are not well reproduced [*Kusahara and Hasumi*, 2013]. This might explain the different pathways of meltwater.

3.3. Sensitivity of Meltwater Transport Into the Ross Sea

We also investigate the sensitivity of basal meltwater transport into the RS associated with the strength of the basal mass loss. In these sensitivity experiments, we increase the basal meltwater flux by a factor k_m, so that

$$F_w = k_m M_{\mathrm{melt}}, \tag{1}$$

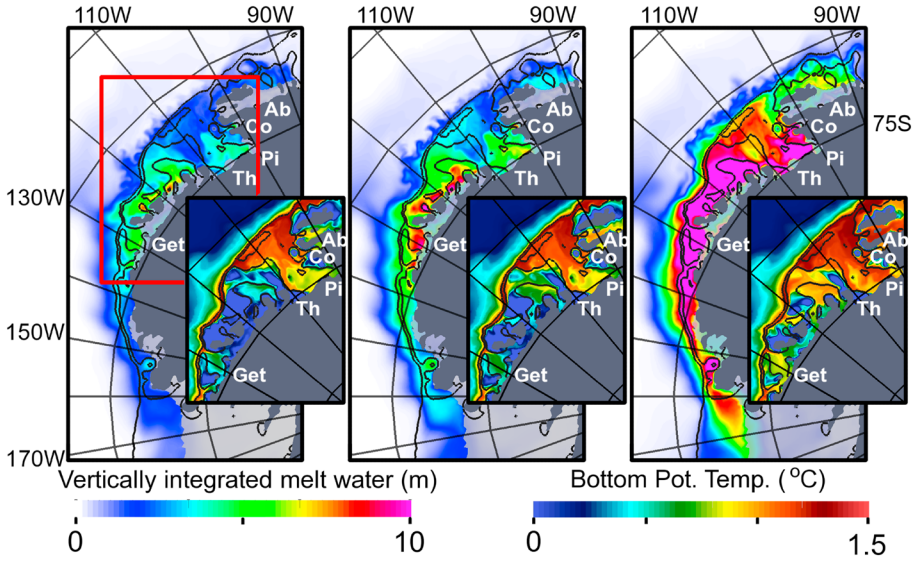

Figure 4. Same as Figure 2 but showing the spatial distributions of the basal meltwater from ice shelves in the AS only for the (a) CTRL (different scale from Figure 2), (b) 1.3 × MELT, and (c) 2.0×MELT cases. The bottom right panels show the bottom potential temperature of the region enclosed by the red line in Figure 4a.

where M_{melt} is the melt rate obtained from the fluxes of heat and salt at the ice shelf base and F_w is the meltwater flux applied to the model ocean at the ice-ocean interface. For the CTRL case, obviously, $k_m = 1$. For the two sensitivity experiments 1.3 × Melt and 2.0 × Melt, we set $k_m = 1.3$ and $k_m = 2.0$, respectively, for all ice shelves in West Antarctica (in the region 140–65°W). In our simulation, we assume that M_{melt} is proportional to $(T_{\mathrm{in}} - T_f)$, where T_{in} and T_f are in situ temperature and in situ freezing point temperature, respectively. Thus, one can associate the increase of k_m with an increase of CDW temperature reaching the ice shelf base. For instance, the case $k_m = 1.3(2.0)$ mimics the situation with CDW temperature 30% (100%) warmer than simulated in the CTRL case. The CDW temperature is ~0.5°C at the Pine Island Ice Shelf front for the CTRL case, and the 1.3 × MELT (2.0 × MELT) case mimics the situation with a CDW temperature of 1.2 (2.8)°C. We note that inflowing CDW temperatures are simulated lower than observations at some of the ice shelf fronts (e.g., observed CDW temperature is ~1.1°C at the Pine Island Ice Shelf front). Therefore, the 1.3 × MELT case may reproduce the situation closer to reality for some AS ice shelves. The total basal mass loss of the AS and BS ice shelves for the 1.3 × MELT case are comparable to the maximum of the observation-based estimates (Table S1 in the supporting information).

In the 1.3 × MELT and 2.0 × MELT cases, more basal meltwater is transported into the RS (Figure 4), and vertically integrated meltwater content is 4–5 times larger in the 2.0 × MELT case than in the CTRL case at the Ross Ice Shelf front, increasing nonlinearly (Figure 4). For the 1.3 × MELT and 2.0 × MELT cases, the meltwater transport quickly increases after the basal mass loss increases. The total amount of basal meltwater transported into the RS is 1.8 (4.9) times more than in the CTRL case by volume after 10 years of simulation (Table S3 in the supporting information), although k_m is set to only 1.3 (2.0) in the 1.3 × MELT (2.0 × MELT) case. This leads to a freshening of 0.1 and 0.4, respectively, at the eastern side of the Ross Ice Shelf front after 10 years of simulation. This indicates that basal meltwater release significantly influences the dynamics of shelf circulation and the transport of basal meltwater into the RS.

If CDW properties intruding into the ice shelf cavities would remain similar to the CTRL case, the basal mass loss of the 1.3 × MELT and 2.0 × MELT cases should be ~1.3 and 2.0 times larger than in the CTRL case, respectively. However, the total combined basal mass loss of AS and BS ice shelves becomes 1.6 and 4.0 times larger for the 1.3 × MELT and 2.0 × MELT cases than for the CTRL case, correspondingly (Table S1 in the supporting information). When bottom potential temperatures of the three cases are compared, ice front bottom temperatures are increasing in most of the regions of the AS (the bottom right panels of Figure 4) and BS (not shown), and the Pine Island Ice Shelf front temperature increases by nearly 0.3°C for the 2.0 × MELT case. This is most likely caused by a strengthening of the shelf circulation and a freshening of the surface waters. The strengthening of the shelf circulation makes CDW intrusions stronger.

For example, annual mean velocities at a depth of 500 m along the pathway of the CDW intrusion from the eastern and central submarine glacial troughs [see *Nakayama et al.*, 2014, Figure 6] both become ~1.5 times and more than 2 times faster for the 1.3 × MELT and 2.0 × MELT cases, respectively. In addition, the freshening of the surface waters weakens the strength of vertical mixing, allowing for a warmer CDW to reach the sub-ice shelf cavities. At the Pine Island Ice Shelf front, mixed layer depth becomes ~50 m and 150 m shallower in winter for the 1.3 × MELT and 2.0 × MELT cases, respectively.

As already mentioned, the total basal meltwater transport into the RS becomes 1.8 and 4.9 times larger for the 1.3 × MELT and 2.0 × MELT cases than in the CTRL case, respectively. This cannot be simply explained by the increase of the basal mass loss alone. Instead, we consider this to be a result of the strengthening of the westward flowing coastal current due to a stronger density gradient (caused by lower shelf salinity) produced by stronger basal melting. For the coastal current crossing 155°W, the mean (averaged for the last 5 years of model simulation) potential densities at a depth of 100 m are 27.3, 27.2, and 27.0 kg m^{-3}, and mean westward velocities are 0.03, 0.04, 0.08 m s^{-1} for the CTRL, 1.3 × MELT, and 2.0 × MELT cases, respectively, confirming the strengthening of coastal current.

Our sensitivity experiments, thus, reveal that a slight increase of the basal mass loss (by warming of inflowing CDW temperature) rapidly intensifies the basal meltwater transport into the RS. The mechanism, which represents a positive feedback, can be summarized as follows. In response to an increase of basal mass loss, the shelf circulation becomes stronger and mixed layer depth becomes shallower due to the surface freshening, leading to the strengthening and warming of CDW intrusions, which again increases the basal mass loss. Further, the larger input of basal meltwater increases the density contrast at the continental shelf break and thus intensifies the coastal current, leading to a more efficient transport of basal meltwater into the RS.

4. Discussion

Based on the time series of averaged shelf water salinity observed in McMurdo Sound and north of Ross Island [*Jacobs and Giulivi*, 2010, Figure 3], salinity remains at ~34.85 between 1958 and 1968 but decreases to ~34.80 for the period 1977–1984. The salinity decreases at a rate of ~0.03 decade $^{-1}$ for 1958–2008 [*Jacobs and Giulivi*, 2010]. A freshening of the 600 m deep RS continental shelf by 0.05, assuming a mean salinity of 34.8, corresponds to a vertically integrated meltwater content increase of ~1 m. Based on our sensitivity experiments, the change of the vertically integrated meltwater content between the CTRL and 1.3 × MELT cases is ~1 m, which is comparable to the magnitude of the freshening observed on the RS continental shelf. In addition, the integrated meltwater contents in the Ross Sea originating from ice shelves in the AS and BS are 1.1×10^3 km^3 and 2.0×10^3 km^3 for the CTRL and 1.3 × MELT cases, respectively, after 10 years of simulation (Table S3 in the supporting information). Thus, the change of the integrated meltwater content in the Ross Sea between the CTRL and 1.3 × MELT cases is 900 km^3. On the other hand, *Comiso et al.* [2011] estimate about 20 km^3 of increased sea ice volume transport out of the Ross Sea every year, leading to a freshwater decrease of 200 km^3 in 10 years. Thus, the increment of freshwater due to basal melting between the CTRL and 1.3 × MELT cases is about 5 times larger than the estimate of increased freshwater export from *Comiso et al.* [2011].

We note that the transport of basal meltwater rapidly increases (in less than 10 years) in response to an increased basal melting in the AS and BS. Thus, considering that mass loss rates of AS and BS ice shelves increased by about 60% between 1996 and 2006 [*Rignot et al.*, 2008], the recent freshening observed on the RS continental shelf may be explained by the positive feedback mechanism proposed in this study. Although no data is available for basal mass loss of AS and BS ice shelves from the 1960s to the 1980s, it is plausible to assume that the earlier RS freshening may go back to the same mechanism. This, in turn, implies that the basal mass loss of the AS ice shelves would have already increased from the 1960s.

5. Summary

It has been suggested that an increased melting of continental ice in the AS and BS is the likely source of the RS freshening [*Jacobs et al.*, 2002; *Jacobs and Giulivi*, 2010]. So far, this hypothesis could not be assessed using numerical models, because it has been difficult to reproduce warm CDW intrusions onto the AS and BS continental shelves in circumpolar or global models. In this study, we reproduce the warm CDW intrusions onto the AS and BS continental shelves and, thus, are able to investigate the spreading of the meltwater of AS and BS ice shelves in the Southern Ocean.

Using virtual passive tracers indicating the ice shelf meltwater fraction per unit ocean volume, we find that basal meltwater from the BS mostly flows westward, toward the AS, but only a small fraction reaches the RS after 10 years of simulation. On the other hand, more than one third of basal meltwater from the AS ice shelves reaches the RS with more than half of the meltwater originating from the Getz Ice Shelf in our simulation. Our results confirm that the basal melting of the ice shelves in the AS could be the reason for the observed RS freshening. Further, our results reveal that a slight increase of the basal mass loss (by warming of the inflowing CDW) can substantially intensify the transport of basal meltwater into the RS as a result of the strengthening of the shelf circulation, the weakening of deep convection due to a freshening of the surface waters, and the acceleration of buoyancy driven coastal current.

Although this study provides one possible explanation for the RS freshening, basal melting of ice shelves is strongly influenced by many factors such as large-scale atmospheric and ocean circulation (which determine the strength and pathway of CDW intrusions), cavity shape, local sea ice formation, issues remaining with continental shelf CDW properties, and basal melting parametrization. Due to the complexity of these processes, our sensitivity experiments, using a uniform increase of the basal mass loss for all the West Antarctic ice shelves, could be too simple. Therefore, further investigation into the reasons for the RS freshening and of the interaction between the different sectors of the Southern Ocean seems necessary.

Acknowledgments

We thank Dmitry Sidorenko and Qiang Wang for their help and support and Shigeru Aoki, Karen M. Assmann, Sergey Danilov, Pierre Dutrieux, Paul Holland, Adrian Jenkins, and Kazuya Kusahara for their useful comments and suggestions. The model code, processing tools, and raw model output are difficult to make publicly available, and the authors recommend contacting the corresponding author for those interested in accessing the data. Insightful comments from two anonymous reviewers were very helpful for the improvement of the paper.

Julienne Stroeve thanks two anonymous reviewers for their assistance in evaluating this paper.

References

Assmann, K., A. Jenkins, D. Shoosmith, D. Walker, S. Jacobs, and K. Nicholls (2013), Variability of circumpolar deep water transport onto the Amundsen Sea continental shelf through a shelf break trough, *J. Geophys. Res. Oceans*, *118*, 6603–6620, doi:10.1002/2013JC008871.

Cavalieri, D., C. Parkinson, P. Gloersen, and H. Zwally (2006), *Sea Ice Concentrations From Nimbus-7 SMMR and DMSP SSM/I Passive Microwave Data*, NSIDC DAAC: NASA DAAC at the National Snow and Ice Data Center, Boulder, Colo.

Comiso, J. C., R. Kwok, S. Martin, and A. L. Gordon (2011), Variability and trends in sea ice extent and ice production in the Ross Sea, *J. Geophys. Res.*, *116*, C04021, doi:10.1029/2010JC006391.

Conkright, M., et al. (2002), World ocean database 2001, volume 1. Introduction, in *NOAA Atlas NESDIS 42*, edited by S. Levitus, 167 pp., US Gov. Print. Off., Washington, D. C.

Corr, H. F., A. Jenkins, K. W. Nicholls, and C. Doake (2002), Precise measurement of changes in ice-shelf thickness by phase-sensitive radar to determine basal melt rates, *Geophys. Res. Lett.*, *29*(8), 73-1–74-4, doi:10.1029/2001GL014618.

Depoorter, M., J. Bamber, J. Griggs, J. Lenaerts, S. Ligtenberg, M. van den Broeke, and G. Moholdt (2013), Calving fluxes and basal melt rates of Antarctic ice shelves, *Nature*, *502*(7469), 89–92.

Dutrieux, P., J. De Rydt, A. Jenkins, P. R. Holland, H. K. Ha, S. H. Lee, E. J. Steig, Q. Ding, E. P. Abrahamsen, and M. Schröder (2014), Strong sensitivity of Pine Island ice-shelf melting to climatic variability, *Science*, *343*(6167), 174–178.

Hellmer, H., and D. Olbers (1989), A two-dimensional model for the thermohaline circulation under an ice shelf, *Antarct. Sci.*, *1*(4), 325–336.

Holland, D. M., and A. Jenkins (1999), Modeling thermodynamic ice-ocean interactions at the base of an ice shelf, *J. Phys. Oceanogr.*, *29*(8), 1787–1800.

Jacobs, S., C. Giulivi, P. Dutrieux, E. Rignot, F. Nitsche, and J. Mouginot (2013), Getz Ice Shelf melting response to changes in ocean forcing, *J. Geophys. Res. Oceans*, *118*, 4152–4168, doi:10.1002/jgrc.20298.

Jacobs, S. S., and C. F. Giulivi (2010), Large multidecadal salinity trends near the Pacific-Antarctic continental margin, *J. Clim.*, *23*(17), 4508–4524.

Jacobs, S. S., C. F. Giulivi, and P. A. Mele (2002), Freshening of the Ross Sea during the late 20th century, *Science*, *297*(5580), 386–389.

Jacobs, S. S., A. Jenkins, C. F. Giulivi, and P. Dutrieux (2011), Stronger ocean circulation and increased melting under Pine Island Glacier ice shelf, *Nat. Geosci.*, *4*(8), 519–523.

Jenkins, A. (1991), A one-dimensional model of ice shelf-ocean interaction, *J. Geophys. Res.*, *96*(C11), 20,671–20,677.

Jenkins, A., and S. Jacobs (2008), Circulation and melting beneath George VI ice shelf, Antarctica, *J. Geophys. Res.*, *113*, C04013, doi:10.1029/2007JC004449.

Kusahara, K., and H. Hasumi (2013), Modeling Antarctic ice shelf responses to future climate changes and impacts on the ocean, *J. Geophys. Res. Oceans*, *118*, 2454–2475, doi:10.1002/jgrc.20166.

Kusahara, K., and H. Hasumi (2014), Pathways of basal meltwater from Antarctic ice shelves: A model study, *J. Geophys. Res. Oceans*, *119*, 5690–5704, doi:10.1002/2014JC009915.

Nakayama, Y., M. Schröder, and H. H. Hellmer (2013), From circumpolar deep water to the glacial meltwater plume on the eastern Amundsen Shelf, *Deep Sea Res. Part I*, *77*, 50–62.

Nakayama, Y., R. Timmermann, M. Schröder, and H. H. Hellmer (2014), On the difficulty of modeling circumpolar deep water intrusions onto the Amundsen Sea continental shelf, *Ocean Model.*, *84*, 26–34.

Potter, J., J. Paren, and J. Loynes (1984), Glaciological and oceanographic calculations of the mass balance and oxygen isotope ratio of a melting ice shelf, *J. Glaciol.*, *30*(105), 161–170.

Pritchard, H. D., S. R. M. Ligtenberg, H. A. Fricker, D. G. Vaughan, M. R. Van den Broeke, and L. Padman (2012), Antarctic ice-sheet loss driven by basal melting of ice shelves, *Nature*, *484*(7395), 502–505.

Rignot, E., J. L. Bamber, M. R. V. den Broeke, C. Davis, Y. Li, W. J. V. de Berg, and E. V. Meijgaard (2008), Recent Antarctic ice mass loss from radar interferometry and regional climate modelling, *Nat. Geosci.*, *1*(2), 106–110.

Rignot, E., S. S. Jacobs, J. Mouginot, and B. Scheuchl (2013), Ice-shelf melting around Antarctica, *Sci. Express*, *341*, 226–270.

Rintoul, S. R. (2007), Rapid freshening of Antarctic bottom water formed in the Indian and Pacific oceans, *Geophys. Res. Lett.*, *34*, L06606, doi:10.1029/2006GL028550.

Rodehacke, C. B., H. H. Hellmer, O. Huhn, and A. Beckmann (2007), Ocean/ice shelf interaction in the southern Weddell Sea: Results of a regional numerical helium/neon simulation, *Ocean Dyn.*, *57*(1), 1–11.

Saha, S., et al. (2010), The NCEP climate forecast system reanalysis, *Bull. Am. Meteorol. Soc.*, *91*(8), 1015–1057.
Schodlok, M. P., D. Menemenlis, E. Rignot, and M. Studinger (2012), Sensitivity of the ice shelf ocean system to the sub-ice shelf cavity shape measured by NASA IceBridge in Pine Island Glacier, West Antarctica, *Ann. Glaciol.*, *53*, 156–162.
Shepherd, A., et al. (2012), A reconciled estimate of ice-sheet mass balance, *Science*, *338*(6111), 1183–1189.
Timmermann, R., and H. H. Hellmer (2013), Southern Ocean warming and increased ice shelf basal melting in the twenty-first and twenty-second centuries based on coupled ice-ocean finite-element modelling, *Ocean Dyn.*, *63*(9–10), 1011–1026.
Timmermann, R., S. Danilov, J. Schröter, C. Böning, D. Sidorenko, and K. Rollenhagen (2009), Ocean circulation and sea ice distribution in a finite element global sea ice–ocean model, *Ocean Model.*, *27*(3), 114–129.
Timmermann, R., et al. (2010), A consistent dataset of Antarctic ice sheet topography, cavity geometry, and global bathymetry, *Earth Syst. Sci. Data*, *2*(2), 261–273.
Timmermann, R., Q. Wang, and H. Hellmer (2012), Ice-shelf basal melting in a global finite-element sea-ice/ice-shelf/ocean model, *Ann. Glaciol.*, *53*(60), 303–314.
Walker, D. P., A. Jenkins, K. M. Assmann, D. R. Shoosmith, and M. A. Brandon (2013), Oceanographic observations at the shelf break of the Amundsen Sea, Antarctica, *J. Geophys. Res. Oceans*, *118*, 2906–2918, doi:10.1002/jgrc.20212.